Electronic Supplementary Material (ESI) for ChemComm.

SUPPLEMENTARY INFORMATION

Chloride-binding in organic-water mixture: the powerful synergy of C-H donor groups within a bowl-shaped cavity

Valeria Amendola,[a]* Greta Bergamaschi,[a] Massimo Boiocchi,[b] Laura Legnani,[a] Eliana Lo Presti,[a] Ana Miljkovic,[a] Enrico Monzani[a] and Francesca Pancotti[a]

[a.] *Department of Chemistry, Università degli Studi di Pavia, via Taramelli 12, Pavia (Italy); e-mail: amendola@unipv.it*

[b.] *Centro Grandi Strumenti, via Bassi 21, Pavia (Italy)*

Index:

1. Experimental

1.1 Materials and methods

All reagents were purchased from Alfa-Aesar and Sigma-Aldrich, and used without further purification. Details of the syntheses are reported in the ESI. Mass spectra were acquired on a Thermo Finnigan ion trap LCQ Advantage Max instrument equipped with an ESI source. ^{1}H-, ^{19}F- and ^{13}C-NMR spectra were recorded on a Bruker ADVANCE 400 spectrometer (operating at 9.37 T, 400 MHz). The experimental procedures of NMR titrations are described elsewhere.[1] Titration data were processed with the Hyperquad package[2] to determine the equilibrium constants.

Crystal structure analysis

Diffraction data for [**1**(Cl)]$(PF_6)_2$·MeCN and [**1**(Br)]$(PF_6)_2$·MeCN isomorphous crystals were collected by means of an Enraf-Nonius CAD4 four circle diffractometer, working at room temperature with MoKα X-radiation (λ = 0.7107 Å). See Tables S1-S2 for details.

Data reductions (including intensity integration, background, Lorentz and polarization corrections) were performed with the WinGX package;[3] absorption effects were evaluated with the psi-scan method[4] and absorption correction was applied to the data.

The crystal structures were solved by direct methods (SIR 97)[5] and refined by full-matrix least-squares procedures on F^2 using all reflections (SHELXL-2014).[6] Anisotropic displacement parameters were used for all non-hydrogen atoms. Hydrogens have been placed at calculated positions and their positions refined according to a riding model.

For both isomorphous crystals, features of the acetonitrile solvent molecules were not clear, probably because of positional disorder that could not be resolved with the available diffraction data. Atoms belonging to the acetonitrile solvent molecule were refined using soft restraints for the molecular geometries and for the atom displacement parameters.

1.2 Synthesis

2,3,4,5-tetrafluorobenzylbromide was purchased from Alfa-Aesar. Other reagents (e.g. tribromomethyl mesitylene) and solvents were purchased from Sigma-Aldrich, and used without further purification. The synthesis of receptor **2**$(PF_6)_3$ is reported elsewhere.[7]

Synthesis of 1$(PF_6)_3$

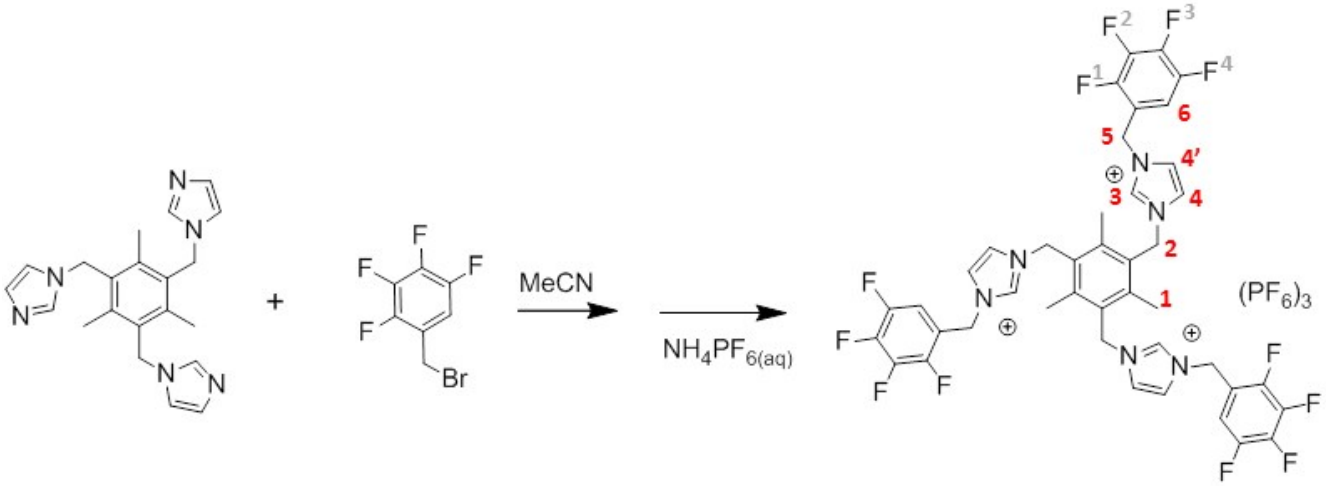

A mixture of 1,3,5-tris(N-imidazolylmethyl)-2,4,6-trimethylbenzene (0.25 g, 0.69 mmol) and 2,3,4,5-tetrafluorobenzylbromide (3.3 eq., 2.27 mmol) in 40 mL MeCN was refluxed for 72 hrs. A white precipitate formed, which was collected by vacuum filtration. The crude tribromide salt was dissolved in the minimum amount of hot water, then treated with a saturated aqueous solution of NH_4PF_6. The solid product **1**$(PF_6)_3$ (0.57 g, 0.45 mmol)) was collected as a white powder by filtration. Yield: 65%

$C_{42}H_{33}N_6P_3F_{30}$: found: C, 39.13; H, 2.63; N, 6.49%, calculated: C, 39.27; H, 2.59; N, 6.54%

ESI-MS (MeOH): m/z 497 [**1**$(PF_6)]^{2+}$, 447 [**1**$(HCOO)]^{2+}$.

^{1}H-NMR (CD_3CN, 400 MHz), δ (ppm): 8.46 (s, 3H, H-3), 7.41 (t, 3H, H-4), 7.35 (t, 3H, H-4'), 7.29 (m, 3H, H-6), 5.45 (s, 6H, H-2), 5.36 (s, 6H, H-5), 2.24 (s, 9H, H-1).
^{13}C-NMR (CD_3CN, 400 MHz), δ (ppm): 142.17 (C-quat), 135.59 (3C, C-H3), 129.38 (C-quat), 123.26 (6C, C-H4', C-H4), 113.3 (C-quat), 112.69 (3C, C-H6), 49.55(3C, C-H2), 46.86 (3C, C-H5), 15.25 (3C, C-H1).
^{19}F-NMR (CD_3CN/CH_3CN 1:1, 400 MHz),), δ (ppm): – 73.2 (d, PF_6^-), – 140.4 (m, F-4), – 143.3 (t, F-1), – 155.8 (t, F-3), – 157.0 (t, F-2).

2. NMR titrations

2.1 pure CD_3CN

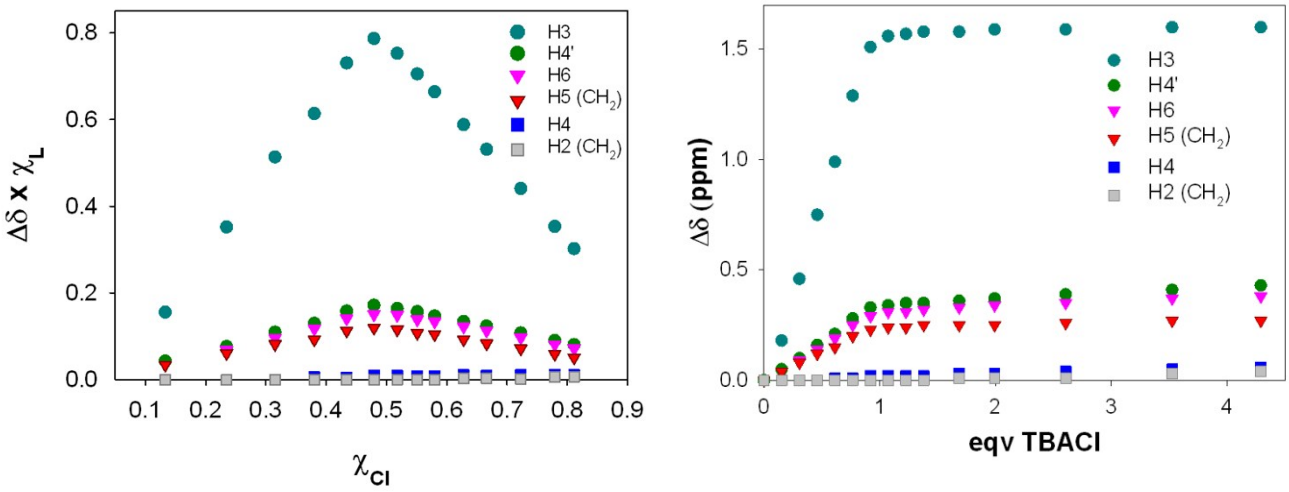

Figure S1: Job plots (left) and profiles (right) of the ^{1}H-NMR titration of **1**$(PF_6)_3$ (1mM) with TBACl in pure CD_3CN.

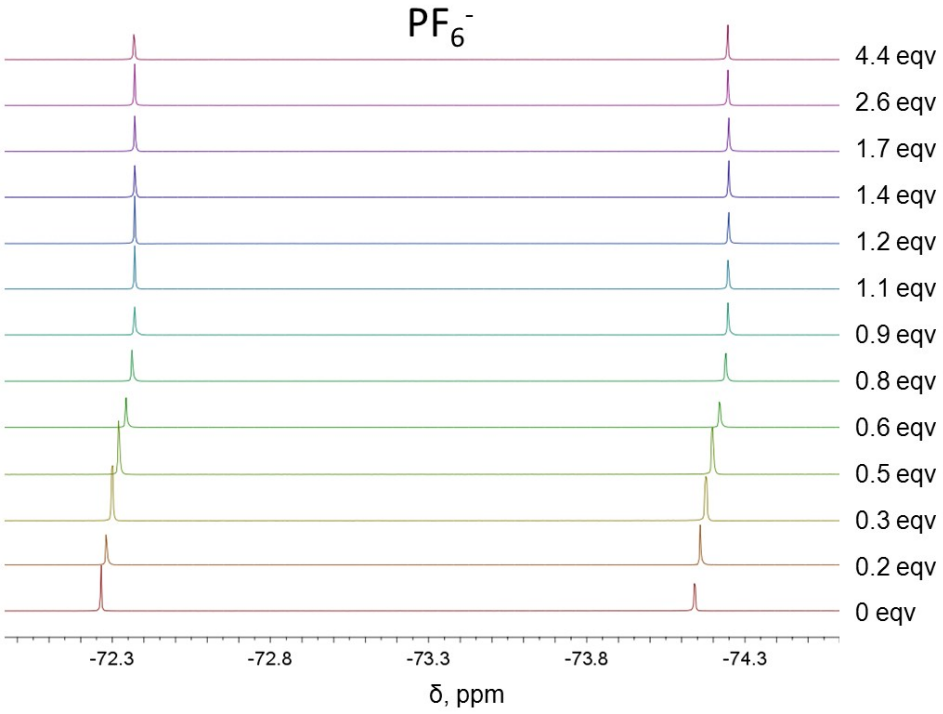

Figure S2: ^{19}F-NMR titration of **1**$(PF_6)_3$ (1 mM) with TBACl in CD_3CN (PF_6^- signal).

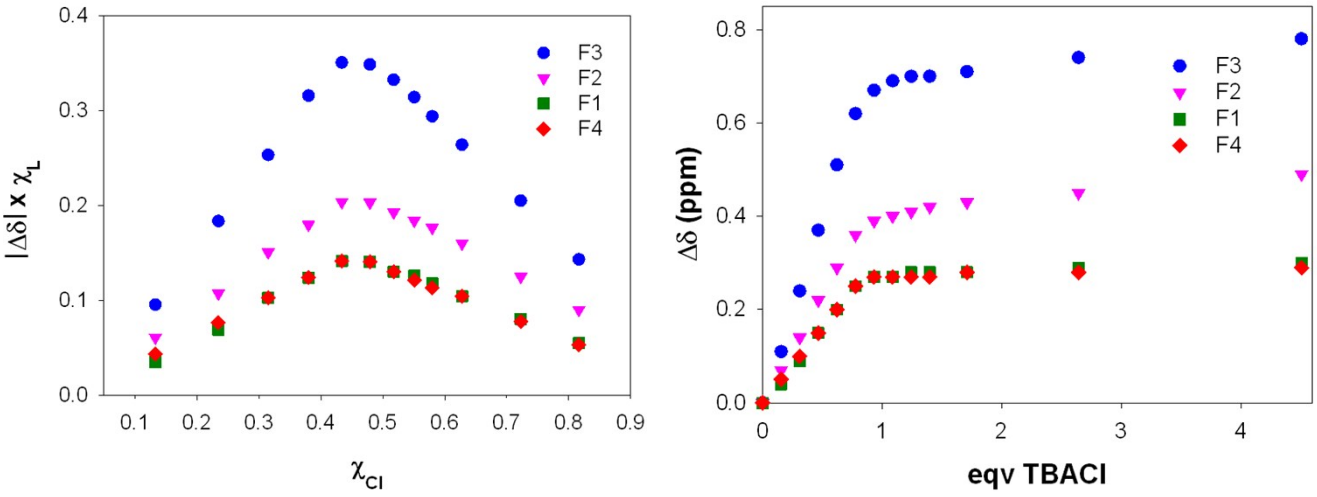

Figure S3: Job plots (left) and profiles (right) of the ^{19}F-NMR titration of **1**$(PF_6)_3$ (1 mM) with TBACl in pure CD_3CN.

2.2 CD_3CN/d^6-DMSO 9:1 and CD_3CN/D_2O 4:1 (v/v) mixtures

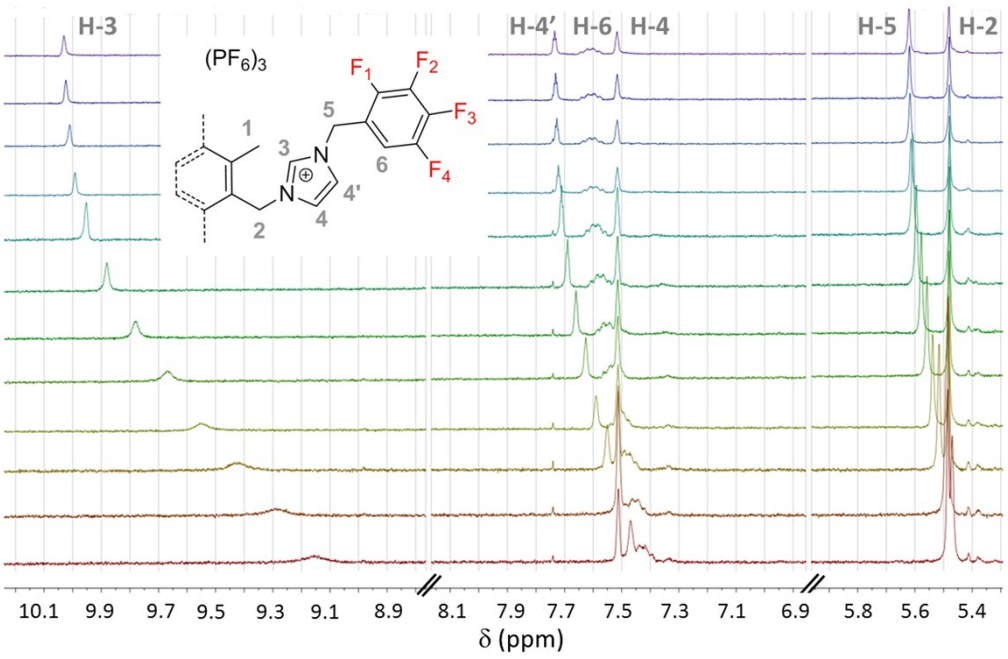

Figure S4: ^{1}H-NMR titration of **1**$(PF_6)_3$ with TBACl in CD_3CN/d^6-DMSO 9:1 (v/v) mixture.

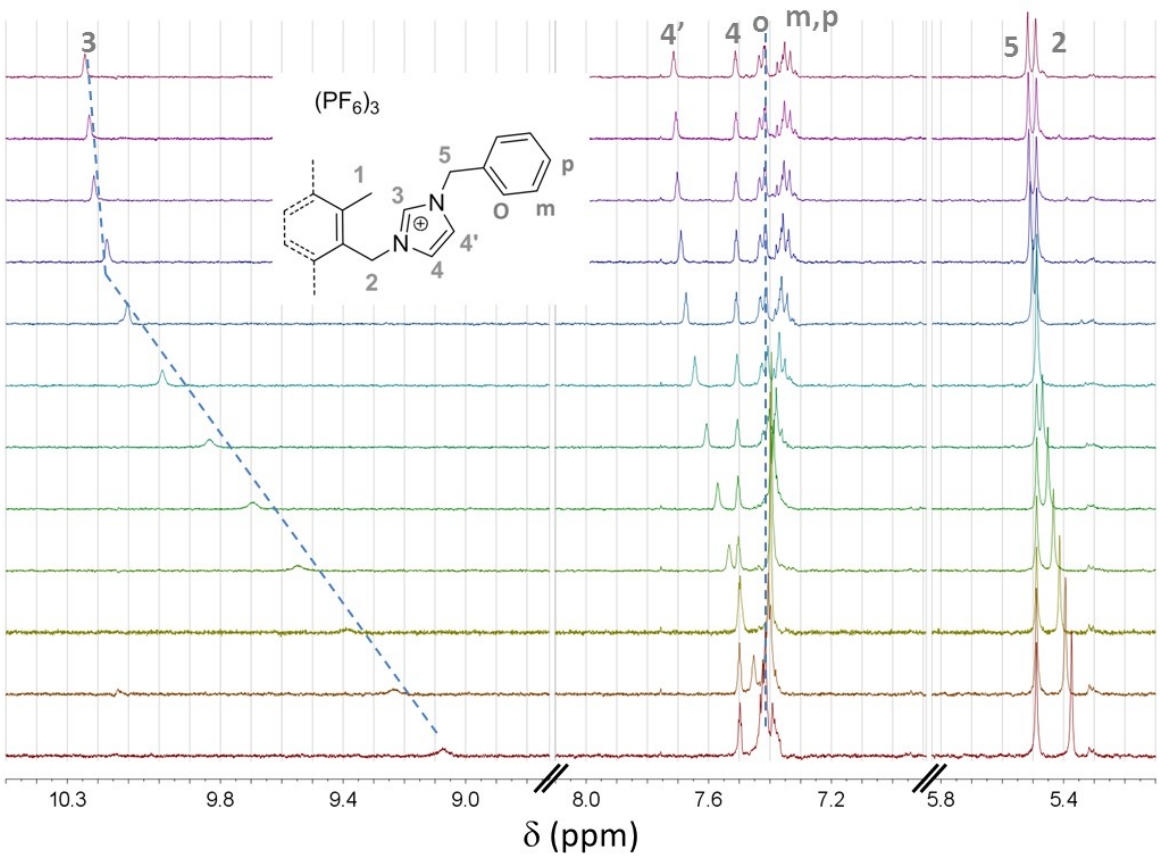

Figure S5: ^{1}H-NMR titration of **2**$(PF_6)_3$ with TBACl in CD_3CN/d^6-DMSO 9:1 (v/v) mixture.

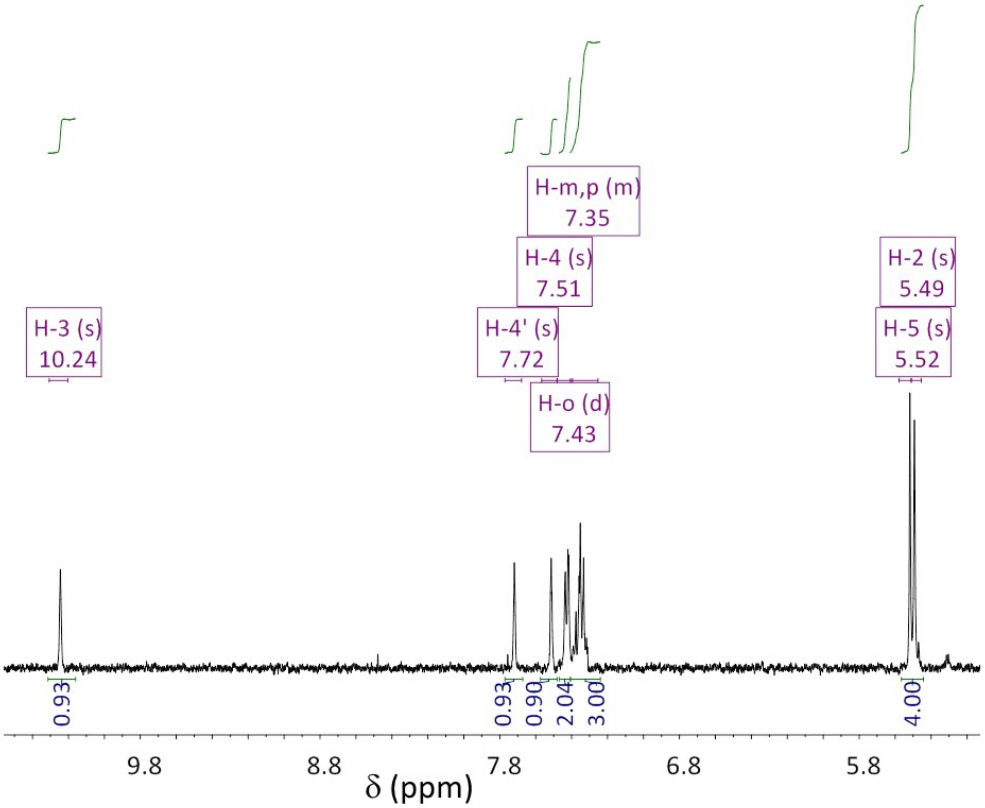

Figure S6: Final ^{1}H-NMR spectrum of the titration of 2$(PF_6)_3$ with TBACl in CD_3CN/d^6-DMSO 9:1 (v/v) mixture.

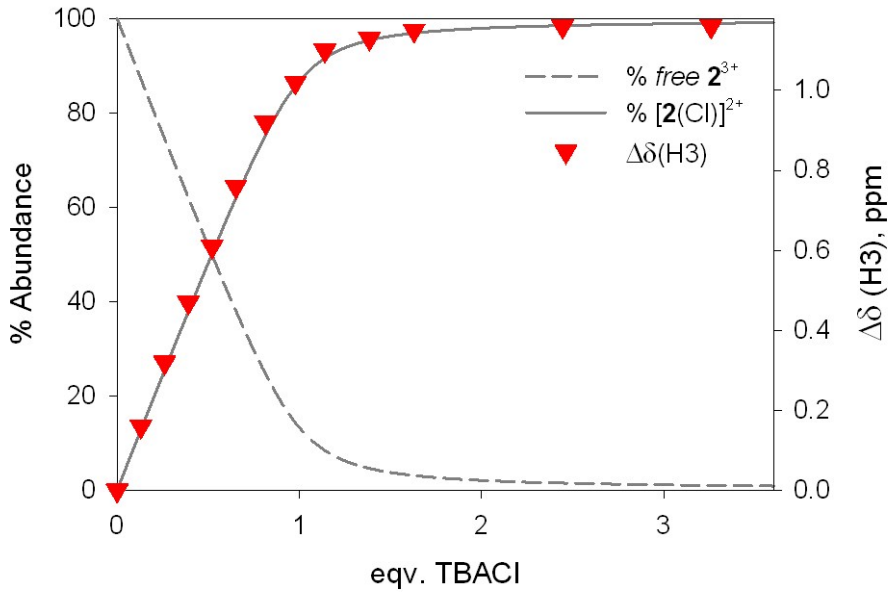

Figure S7: ^{1}H-NMR titration of **2**$(PF_6)_3$ (0.31 mM) with TBACl in CD_3CN/d^6-DMSO mixture (10%v. d^6-DMSO). Distribution diagram of the species in solution, obtained for a binding constant of 5.11(7) log units, superimposed to the experimental plot of Δδ (ppm) vs. eqv. TBACl for protons H-3.

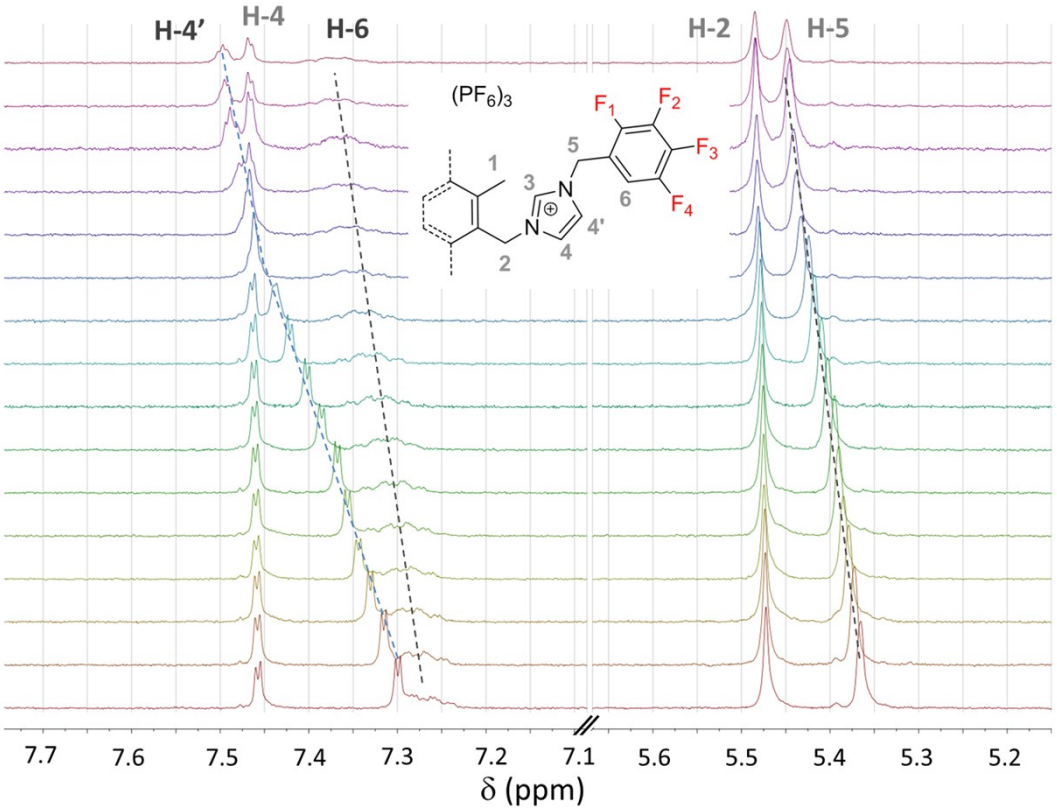

Figure S8: ^{1}H-NMR titration of **1**$(PF_6)_3$ with TBACl in CD_3CN/D_2O 4:1 mixture.

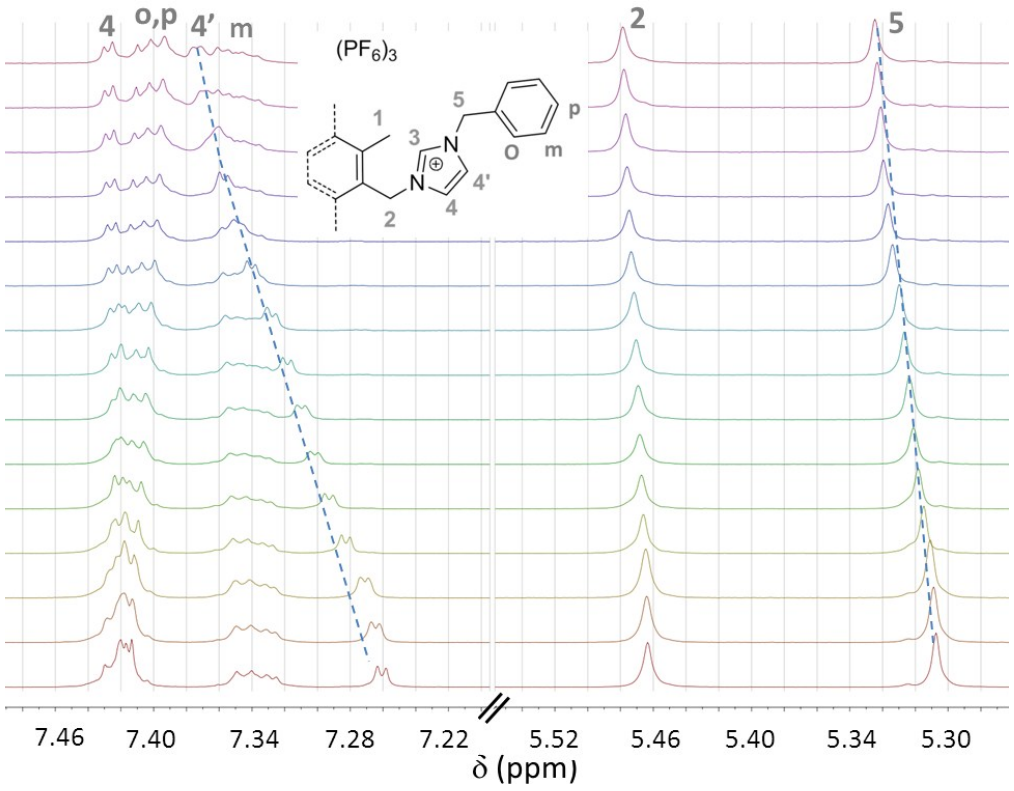

Figure S9: ^{1}H-NMR titration of **2**$(PF_6)_3$ with TBACl in CD_3CN/D_2O 4:1 mixture (see Fig.s S25-S26 for more details).

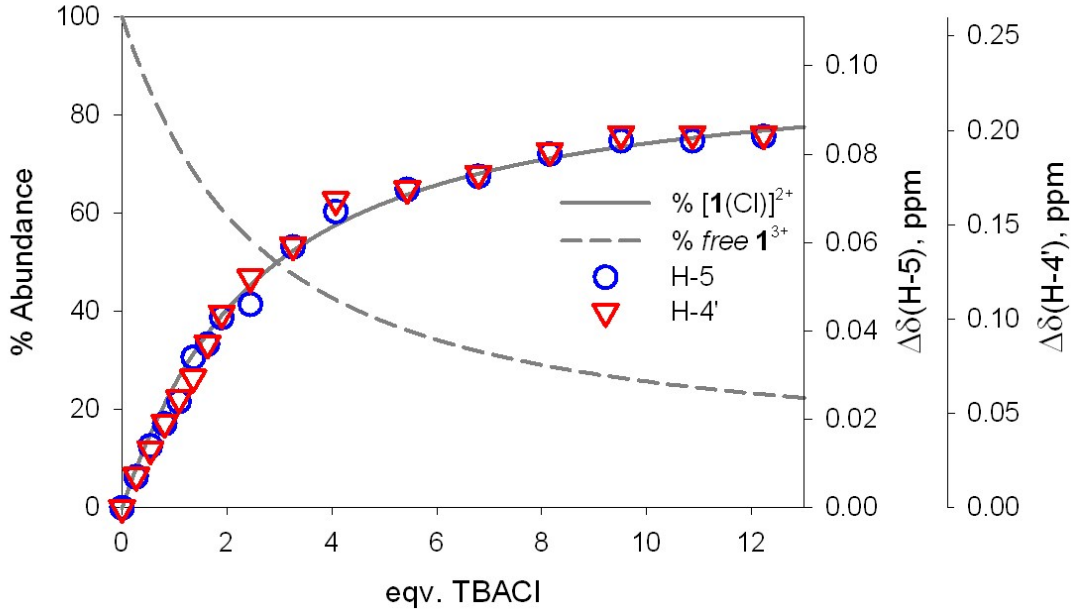

Figure S10: ^{1}H-NMR titration of **1**$(PF_6)_3$ (0.5 mM) with TBACl in CD_3CN/D_2O 4:1 mixture. Distribution diagram of the species in solution, obtained for a binding constant of 3.37(7) log units, superimposed to the experimental plot of Δδ (ppm) vs. eqv. TBACl for protons H-5 and H-4'.

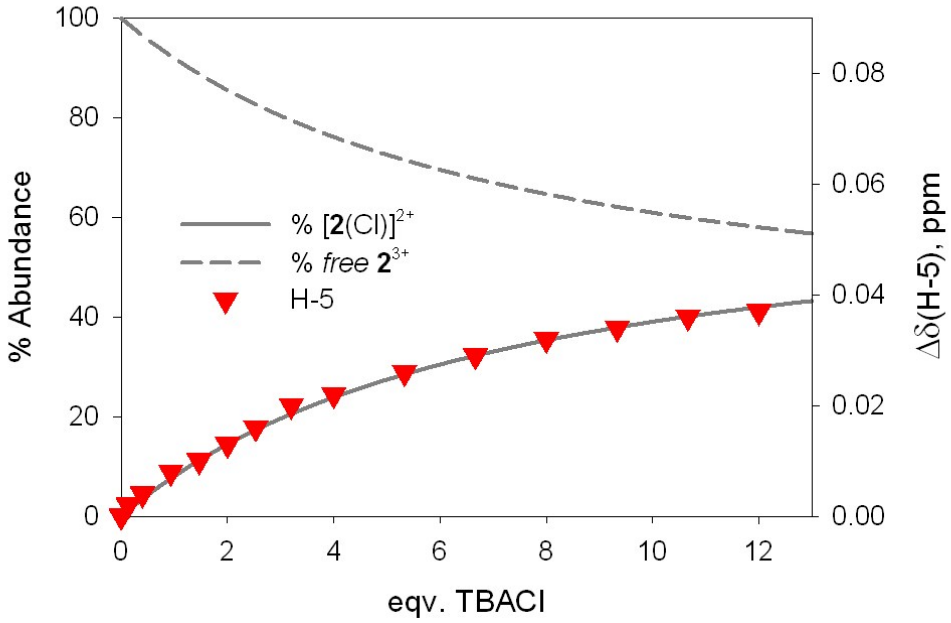

Figure S11: ^{1}H-NMR titration of **2**$(PF_6)_3$ (1.0 mM) with TBACl in CD_3CN/D_2O 4:1 mixture. Distribution diagram of the species in solution, obtained for a binding constant of 2.17(4) log units, superimposed to the experimental plot of Δδ (ppm) vs. eqv. TBACl for protons H-5.

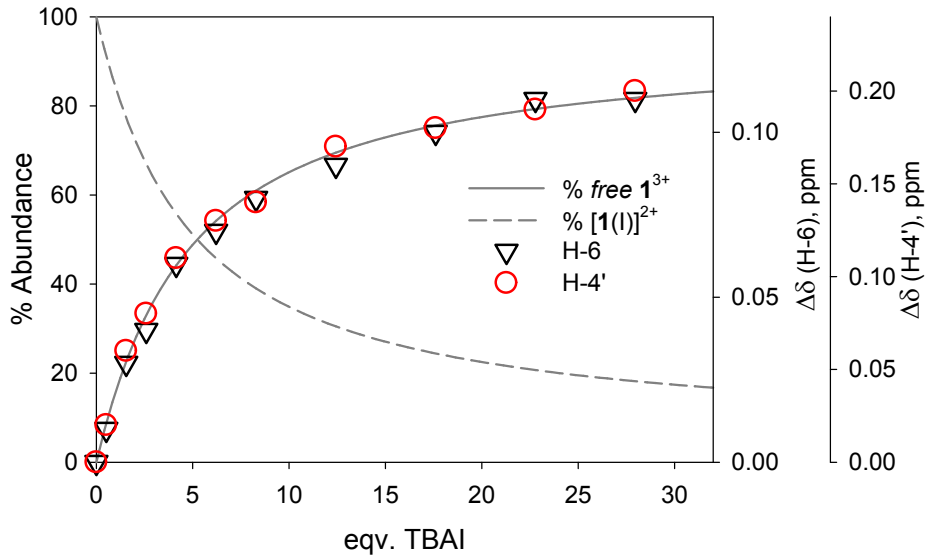

Figure S12: ^{1}H-NMR titration of **1**$(PF_6)_3$ (1.0 mM) with TBAI in CD_3CN/D_2O 4:1 mixture. Distribution diagram of the species in solution, obtained for a binding constant of 2.34(3) log units, superimposed to the experimental plot of Δδ (ppm) vs. eqv. TBACl for protons H-6 and H-4'.

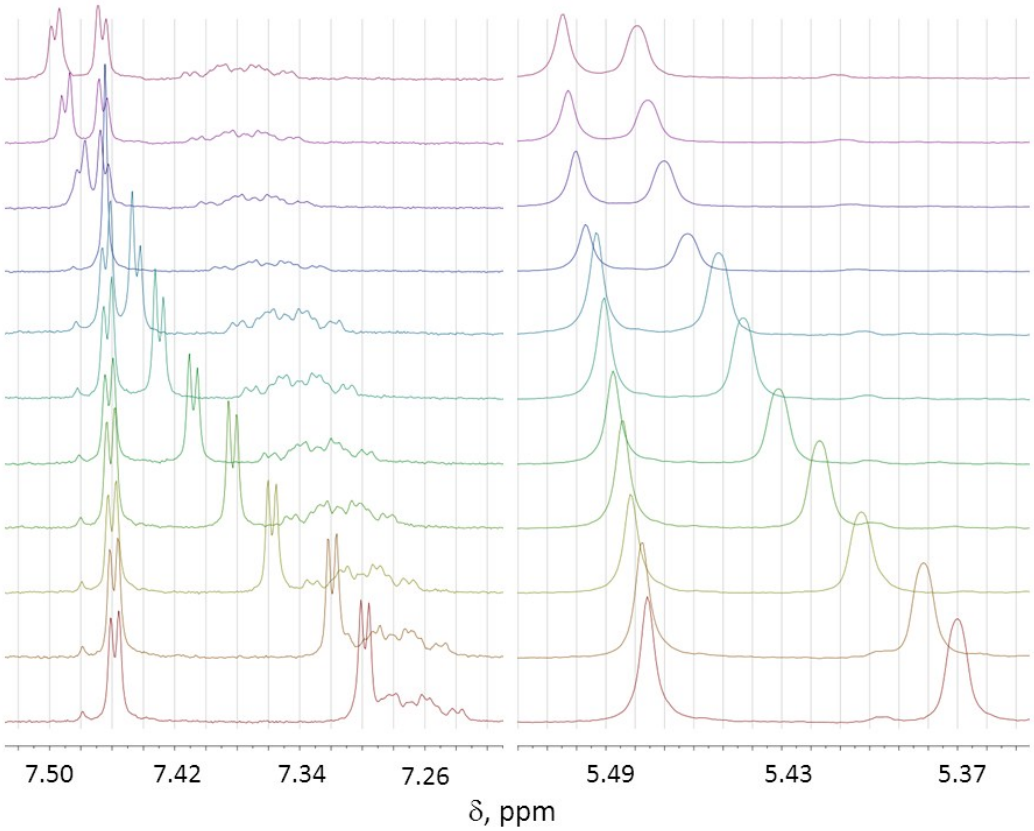

Figure S13: ^{1}H-NMR titration of **1**$(PF_6)_3$ with TBAI in CD_3CN/D_2O 4:1 mixture.

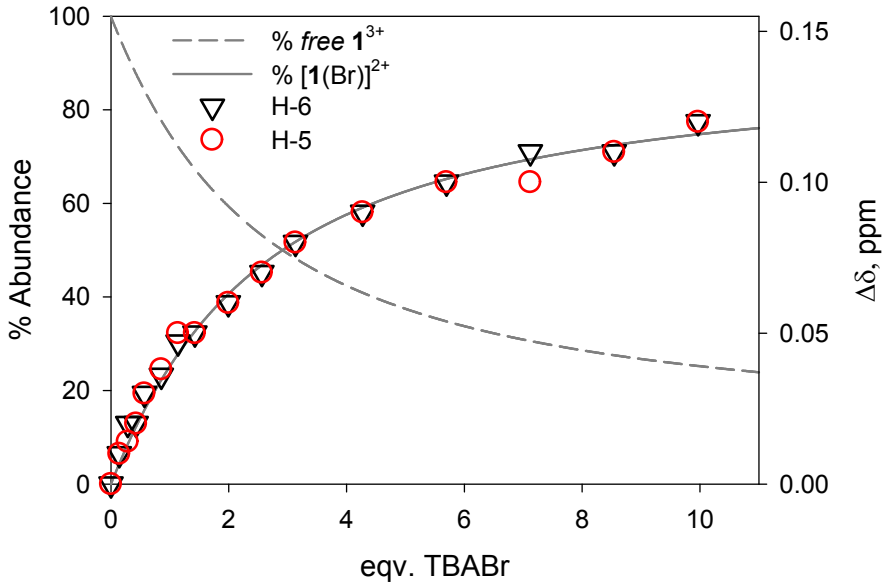

Figure S14: ^{1}H-NMR titration of **1**$(PF_6)_3$ (1.0 mM) with TBABr in CD_3CN/D_2O 4:1 mixture. Distribution diagram of the species in solution, obtained for a binding constant of 2.66(3) log units, superimposed to the experimental plot of Δδ (ppm) vs. eqv. TBACl for protons H-6 and H-5.

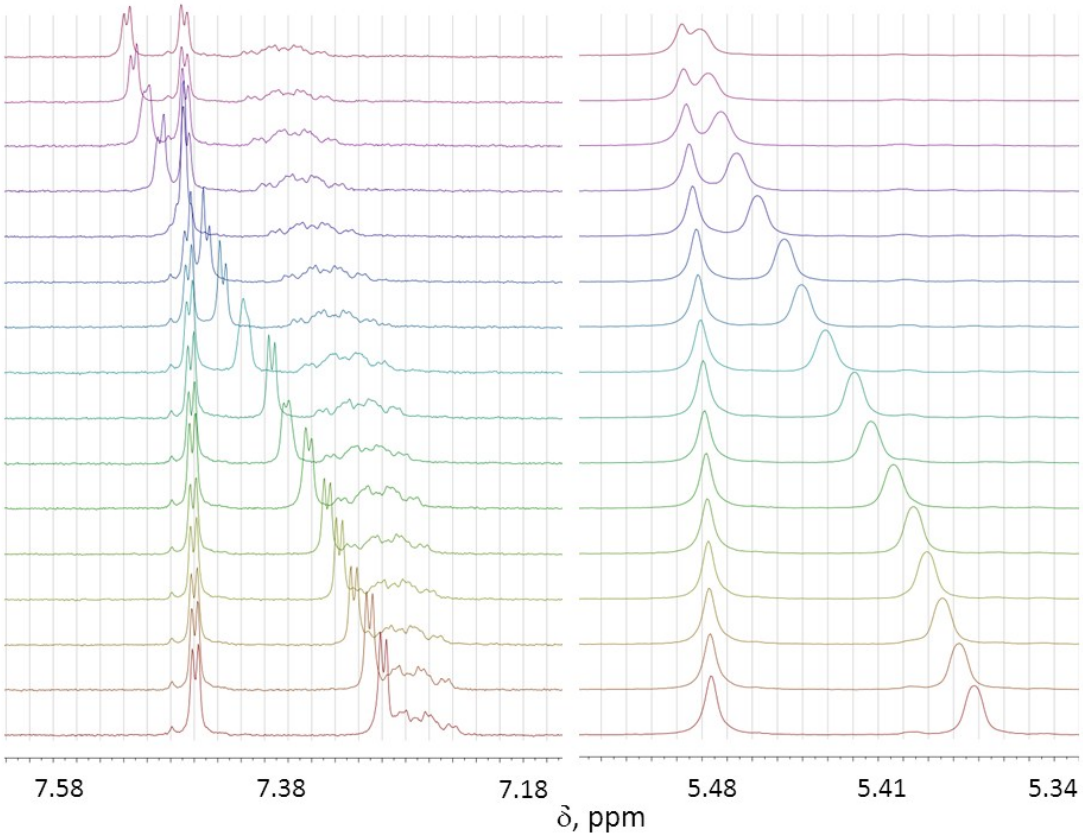

Figure S15: ^{1}H-NMR titration of **1**$(PF_6)_3$ with TBABr in CD_3CN/D_2O 4:1 mixture (see Figs. S23-S24 for more details).

3. X-Ray diffraction studies

	[**1**(Cl)](PF$_6$)$_2$·MeCN	[**1**(Br)](PF$_6$)$_2$·MeCN
Formula	$C_{44}H_{36}ClF_{24}N_7P_2$	$C_{44}H_{36}BrF_{24}N_7P_2$
M [g/mol]	1216.19	1260.64
Dimension [mm]	0.50x0.43x0.14	0.58x0.50x0.38
colour	colourless	colourless
Crystal system	triclinic	triclinic
Space group	*P* -1 (no. 2)	*P* -1 (no. 2)
a [Å]	12.175(4)	12.226(4)
b [Å]	12.483(5)	12.514(2)
c [Å]	18.276(5)	18.219(3)
α [°]	75.34(3)	75.48(1)
β [°]	78.55(2)	78.59(1)
γ [°]	71.31(2)	71.71(2)
V [Å^3]	2524.5(15)	2540.5(11)
Z	2	2
ρ_{calcd} [g/cm^3]	1.600	1.648
μ Mo K_α [mm-^{1}]	0.269	1.002
diffractometer type	Enraf-Nonius CAD4	Enraf-Nonius CAD4
detector type	scintillation counter	scintillation counter
θ range [°]	2-25	2-25
Measured refl.	8913	8948
Unique refl.	8913	8948
R_{int}*	-	-
min/max transmission	0.88/0.96	0.65/0.70
Strong data ($I_0>2\sigma(I_0)$)	4693	7877
Refined parameters	707	707
R1, *wR2* (strong data)	0.1227, 0.2647	0.0777, 0.0850
R1, *wR2* (all data)	0.1804, 0.3054	0.2031, 0.2115
GOF	1.062	1.062
Max/min resid. [eÅ^{-3}]	0.78/-0.44	1.12/-0.57

*centrosymmetrically related reflections were not collected

Table S1: Details on the crystal structures of [**1**(Cl)](PF$_6$)$_2$·MeCN and [**1**(Br)](PF$_6$)$_2$·MeCN.

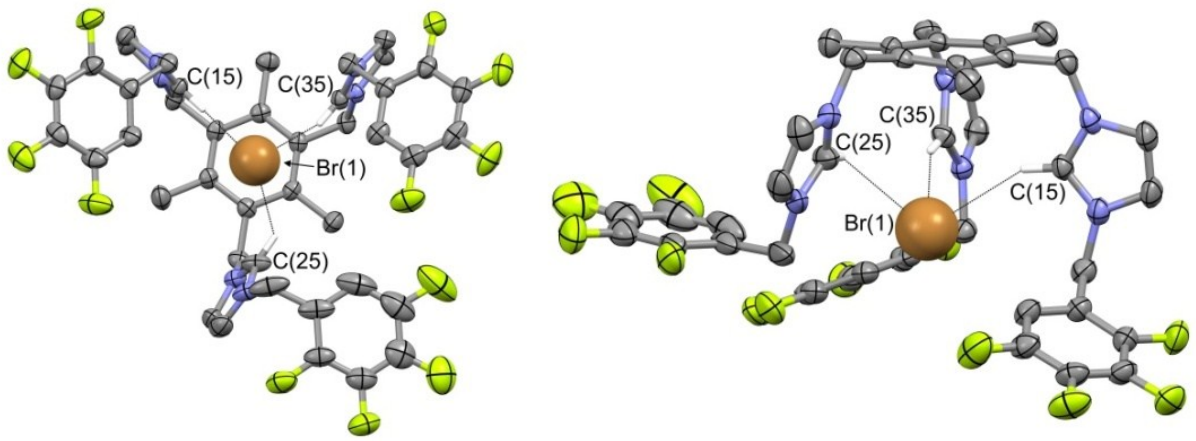

Figure S16: Top (above) and lateral (below) views of the molecular cation $\mathbf{1}^{3+}$ interacting with bromide (additional PF_6^- counterions and MeCN solvent molecules have been omitted for clarity). Atom names are only reported for atoms involved in C-H···Br$^-$ hydrogen bonds, drawn with black [2.68(1)<H···Br$^-$<2.75(1) Å] and grey [2.94(1)<H···Br$^-$<3.15(1) Å] dashed lines.

Donor group	**C···A$^-$ (Å)**	**H···A$^-$ (Å)**	**C–H···A$^-$ (°)**	**A acceptor atom**
C(15)-H(15)	3.494(8)	2.659(8)	149.7(8)	Cl(1)
C(25)-H(25)	3.273(9)	2.555(9)	134.3(9)	Cl(1)
C(35)-H(35)	3.420(8)	2.568(8)	152.5(9)	Cl(1)
C(16)-H(16)b	3.675(9)	2.817(9)	147.9(9)	Cl(1)
C(22)-H(22)	3.854(10)	3.017(10)	150.5(11)	Cl(1)
C(26)-H(26)b	3.707(11)	2.882(11)	143.5(12)	Cl(1)
C(36)-H(36)a	3.829(9)	3.023(9)	141.4(10)	Cl(1)
C(42)-H(42)	3.935(10)	3.092(10)	151.6(11)	Cl(1)
C(15)-H(15)	3.578(5)	2.733(5)	151.4(3)	Br(1)
C(25)-H(25)	3.367(7)	2.751(7)	124.5(4)	Br(1)
C(35)-H(35)	3.540(5)	2.683(5)	153.6(3)	Br(1)
C(16)-H(16)b	3.807(6)	2.966(6)	145.7(4)	Br(1)
C(22)-H(22)	3.902(6)	3.058(6)	151.7(4)	Br(1)
C(26)-H(26)b	3.763(7)	2.940(7)	143.4(5)	Br(1)
C(36)-H(36)a	3.926(6)	3.105(6)	143.2(4)	Br(1)
C(42)-H(42)	4.005(7)	3.149(7)	154.0(5)	Br(1)

Table S2: Geometrical features for the C–H···Cl$^-$ and C–H···Br$^-$ hydrogen-bonds.

4 Computational Methods

All the calculations were carried out using the GAUSSIAN09 program package. All the structures were optimized in the gas phase at the B3LYP/6-311+G(2df,p) level for the Cl atom and 6-311+G(d,p) level for the other atoms. NBO analysis was performed at the same level of calculations.[8]

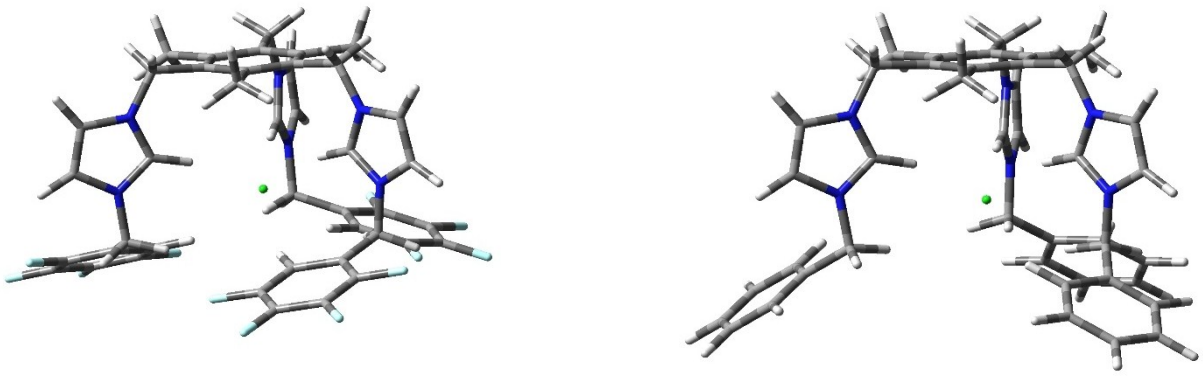

Figure S17: Three-dimensional plots of the preferred conformations of **[1**(Cl)]$^{2+}$ (left) and **[2**(Cl)]$^{2+}$ (right).

distances	[**1**(Cl)]$^{2+}$	[**2**(Cl)]$^{2+}$
C3···Cl$^-$ (Å)	3.415	3.347
C5···Cl$^-$ (Å)	4.112	3.946
C6···Cl$^-$ (Å)	3.703	5.230
NPA charges	*free* **1**$^{3+}$	*free* **2**$^{3+}$
H3	0.227	0.228
H5a	0.224	0.206
H6	0.206	0.193
ESP values		
H3	+0.367	+0.351
H5	+0.306	+0.297
H6	+0.328	+0.273

Table S3: C···Cl$^-$ distances (Å) in [**1**(Cl)]$^{2+}$ and [**2**(Cl)]$^{2+}$ complexes; corresponding NPA charges and MEP values for the H atoms in the free ligands **1**$^{3+}$ and **2**$^{3+}$.

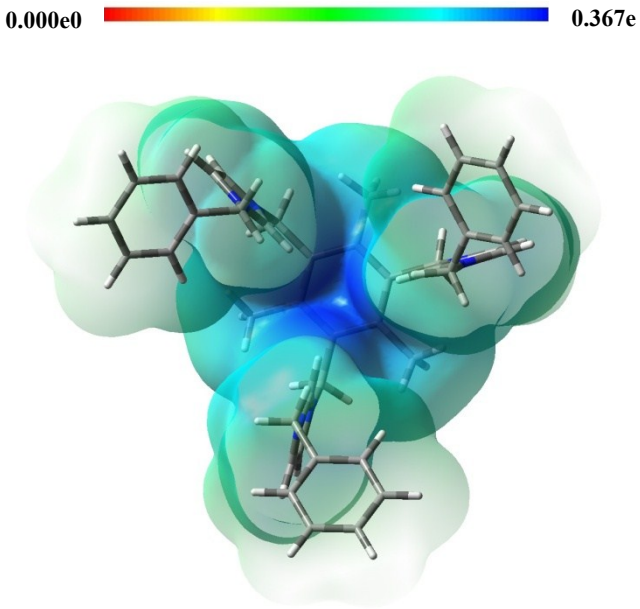

Figure S18: Molecular Electrostatic Potential (MEP) surface of the receptor in the complex **2**/Cl^- (transparent representation). The anion is omitted for clarity.

5 Characterization

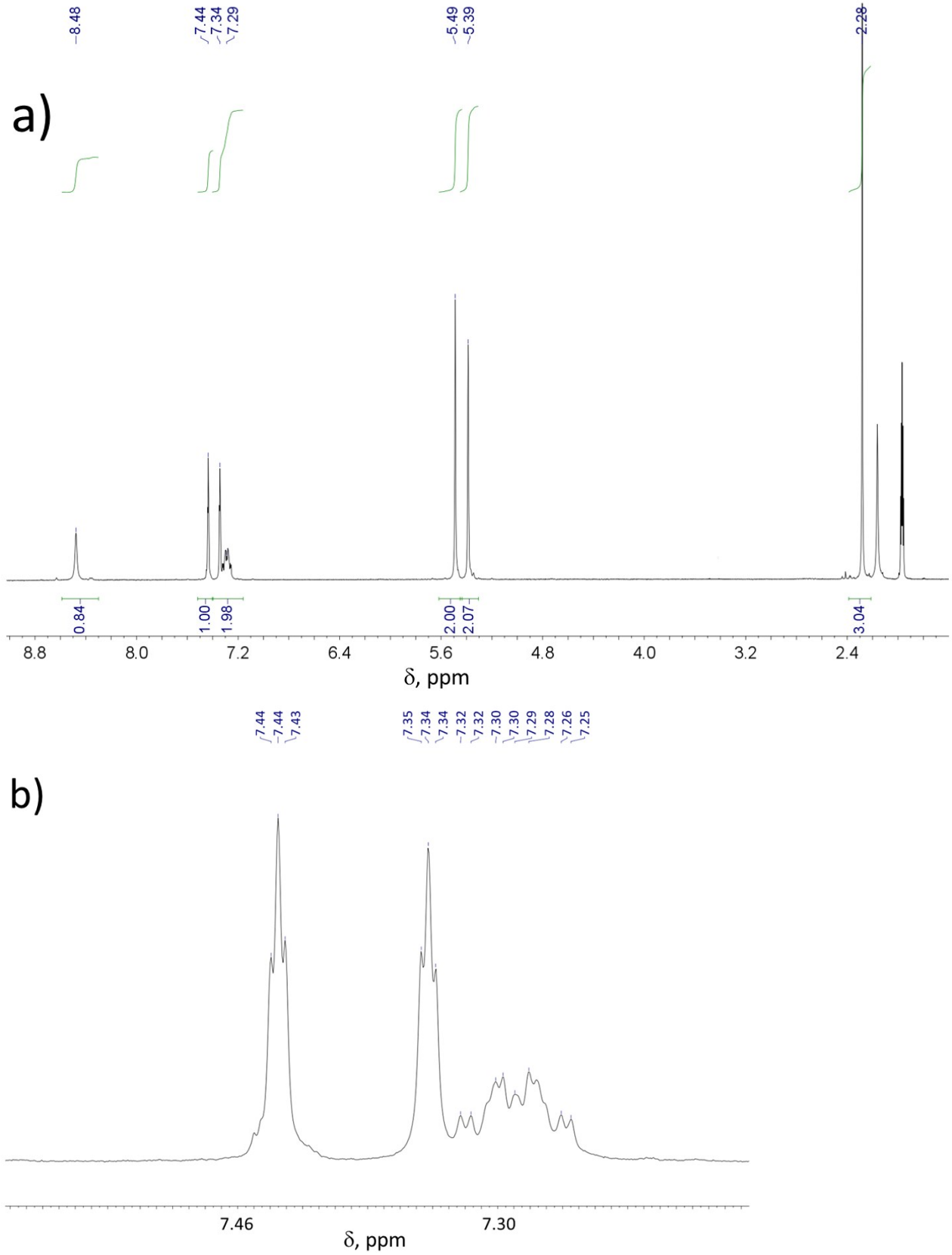

Figure S19: ^{1}H-NMR spectrum of **1**$(PF_6)_3$ in CD_3CN: a) full spectrum; b) enlargement: $\Delta\delta$ = 7.50 – 7.19 ppm

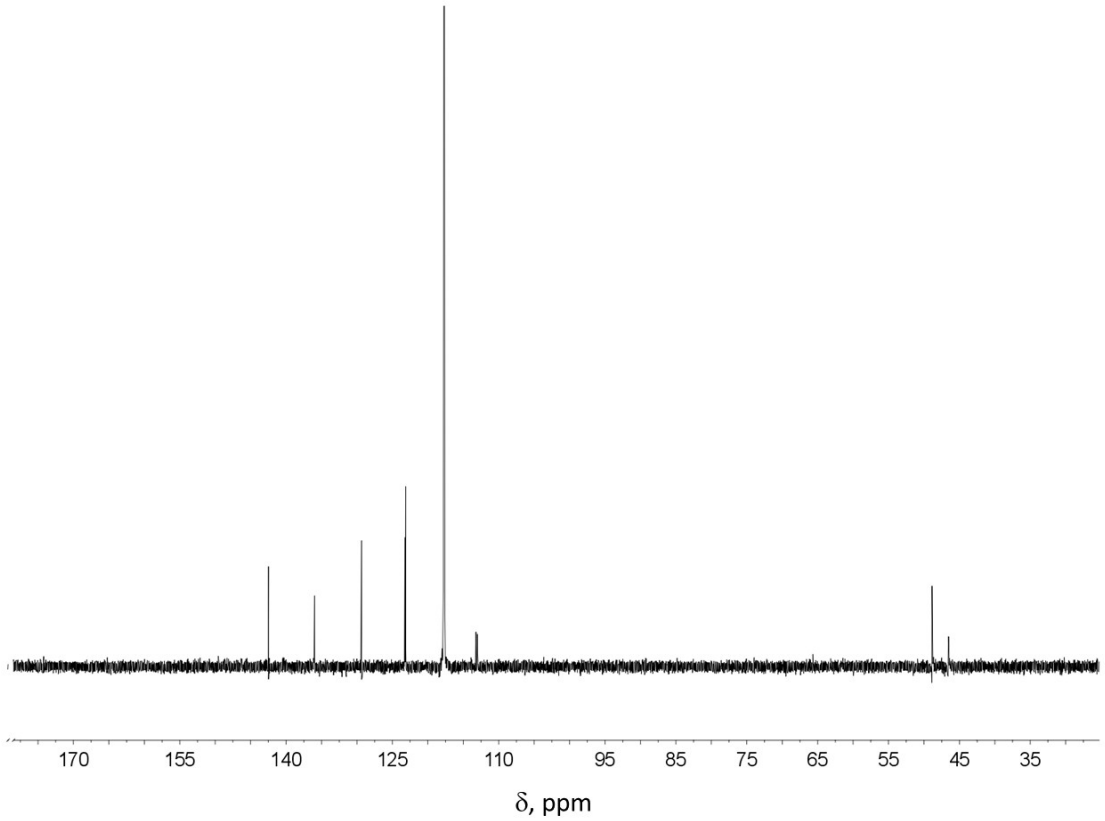

Figure S20: ^{1}H-decoupled ^{13}C-NMR spectrum of **1**$(PF_6)_3$ in CD_3CN

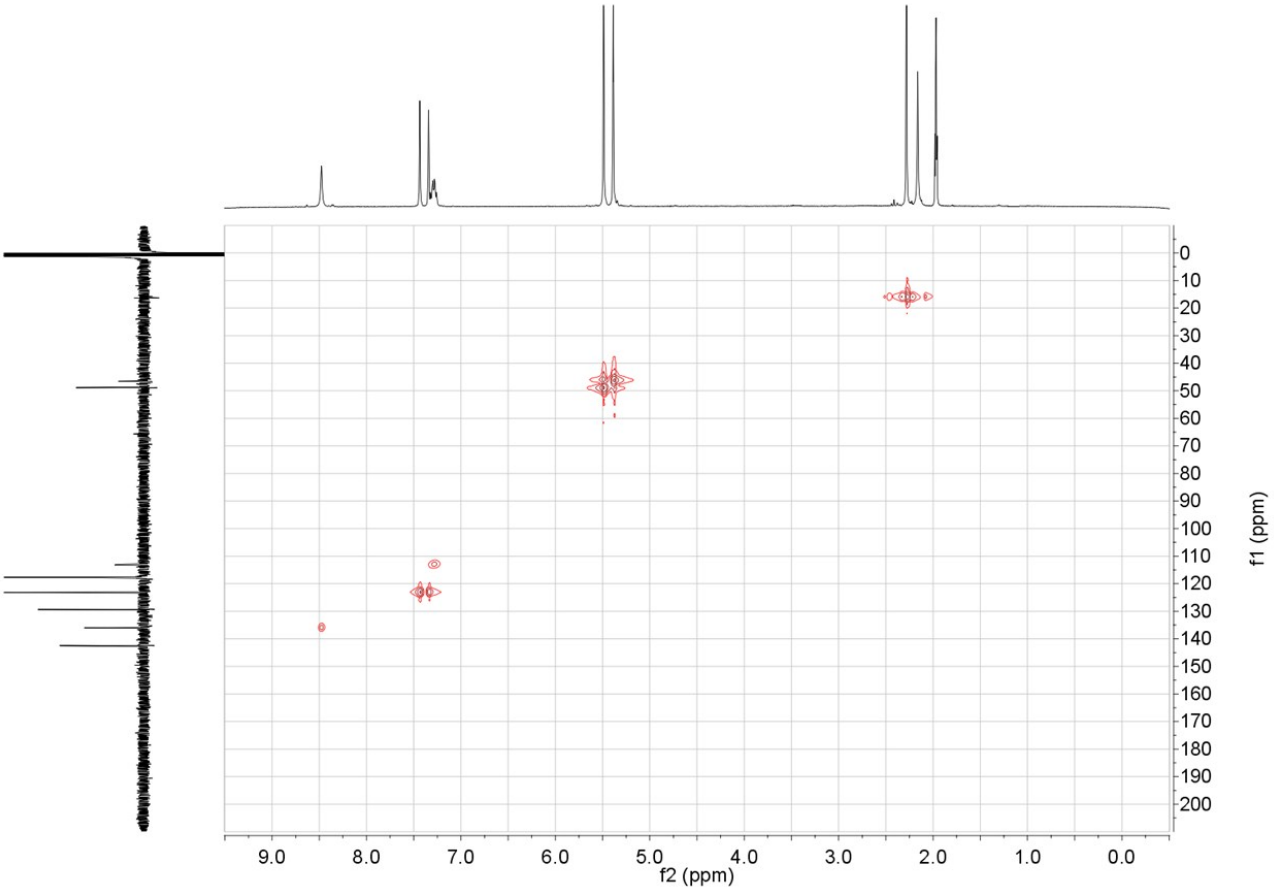

Figure S21: 2D-HSQC spectra of **1**$(PF_6)_3$ in CD_3CN

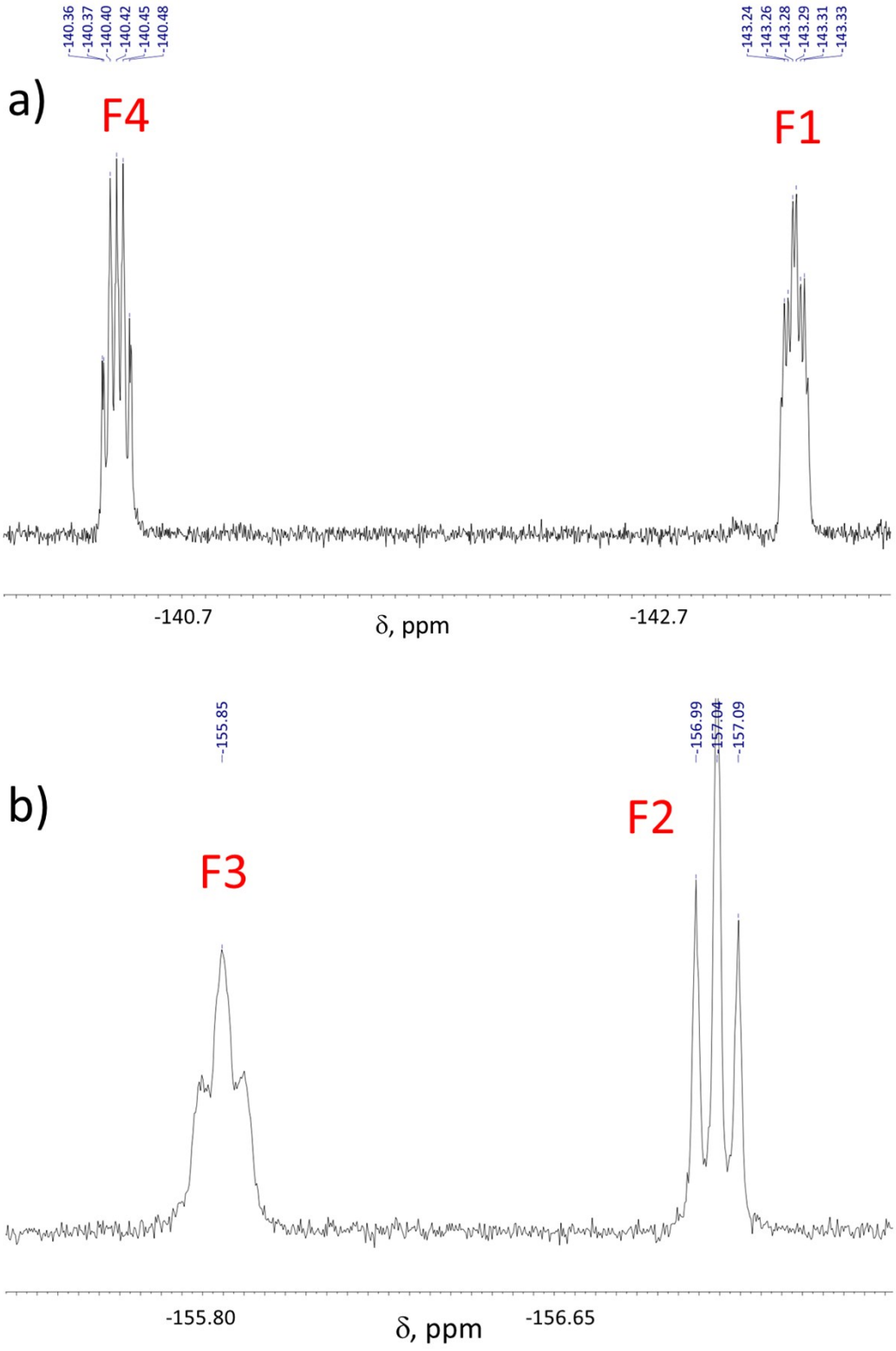

Figure S22: ^{19}F-NMR spectrum of **1**$(PF_6)_3$ in CD_3CN: details of fluorine signals

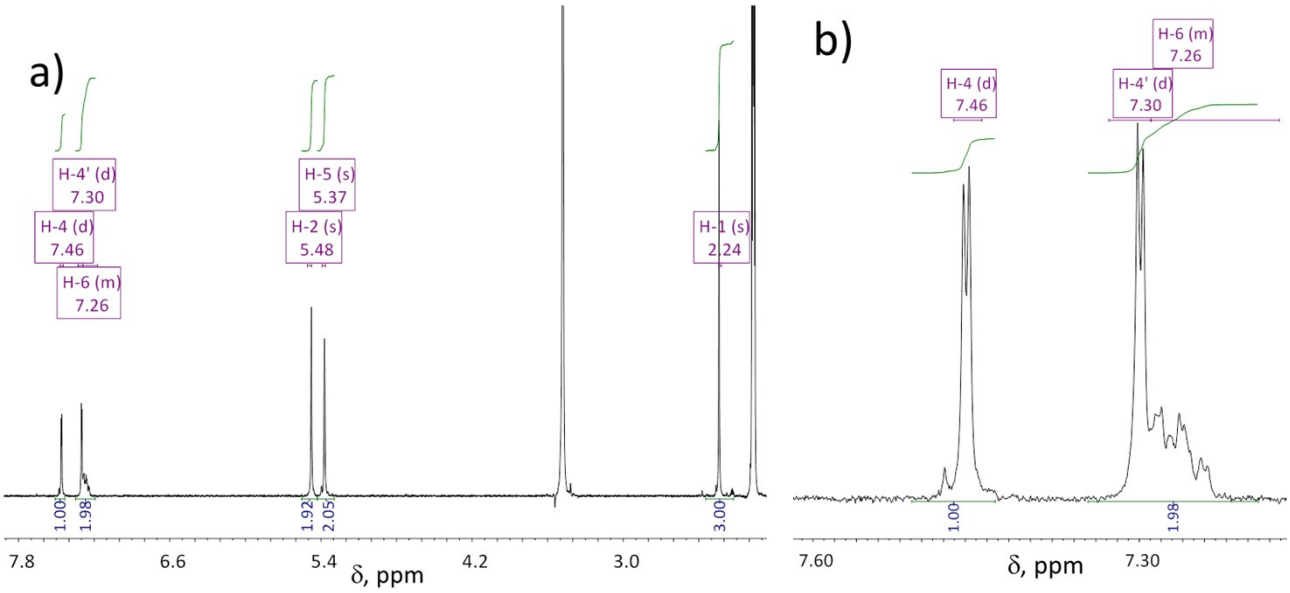

Figure S23: ^{1}H-NMR spectrum of **1**$(PF_6)_3$ in CD_3CN/D_2O 4:1 (initial spectrum of the titration reported in Fig. S15): a) full spectrum, b) zoom of the aromatic region.

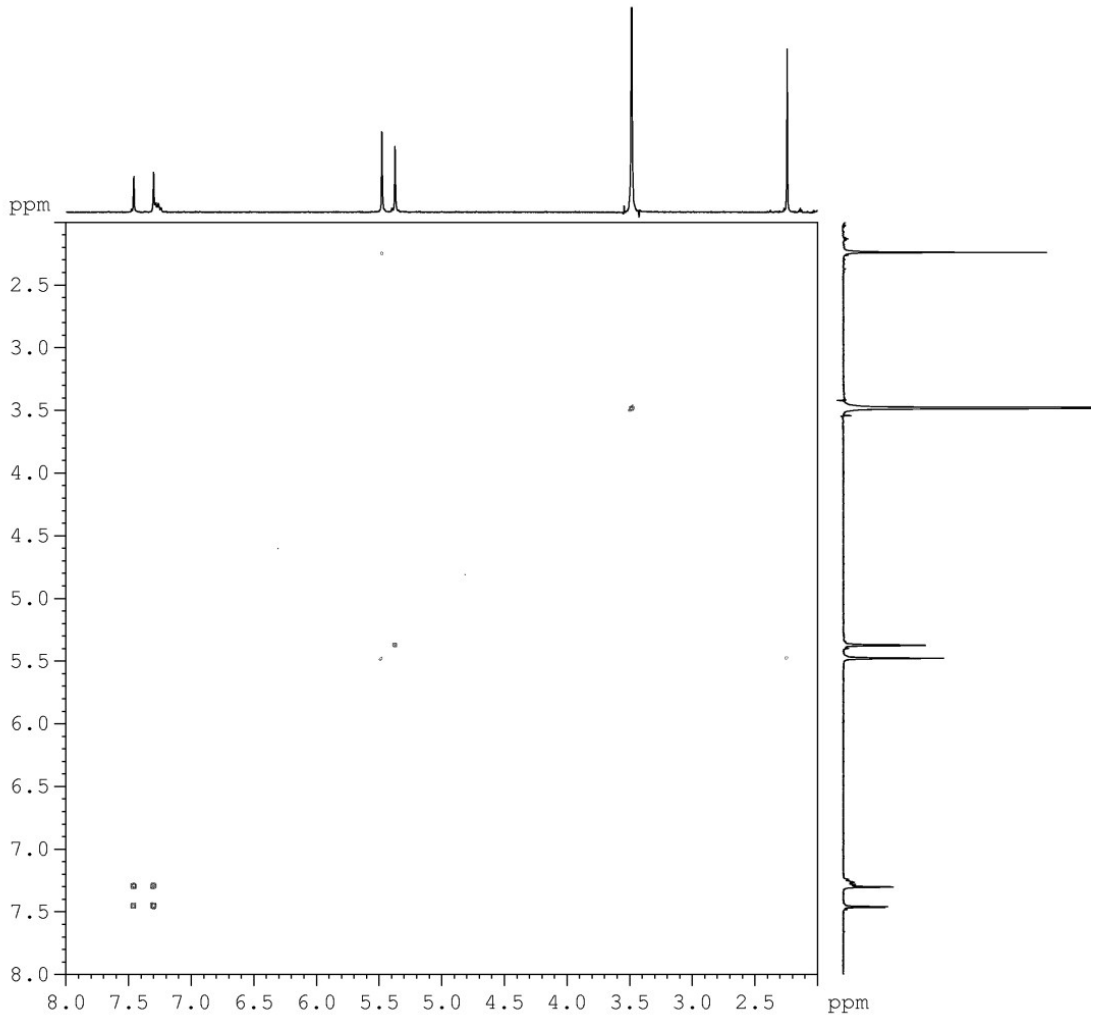

Figure S24: COSY spectrum of **1**$(PF_6)_3$ in CD_3CN/D_2O 4:1(v/v)

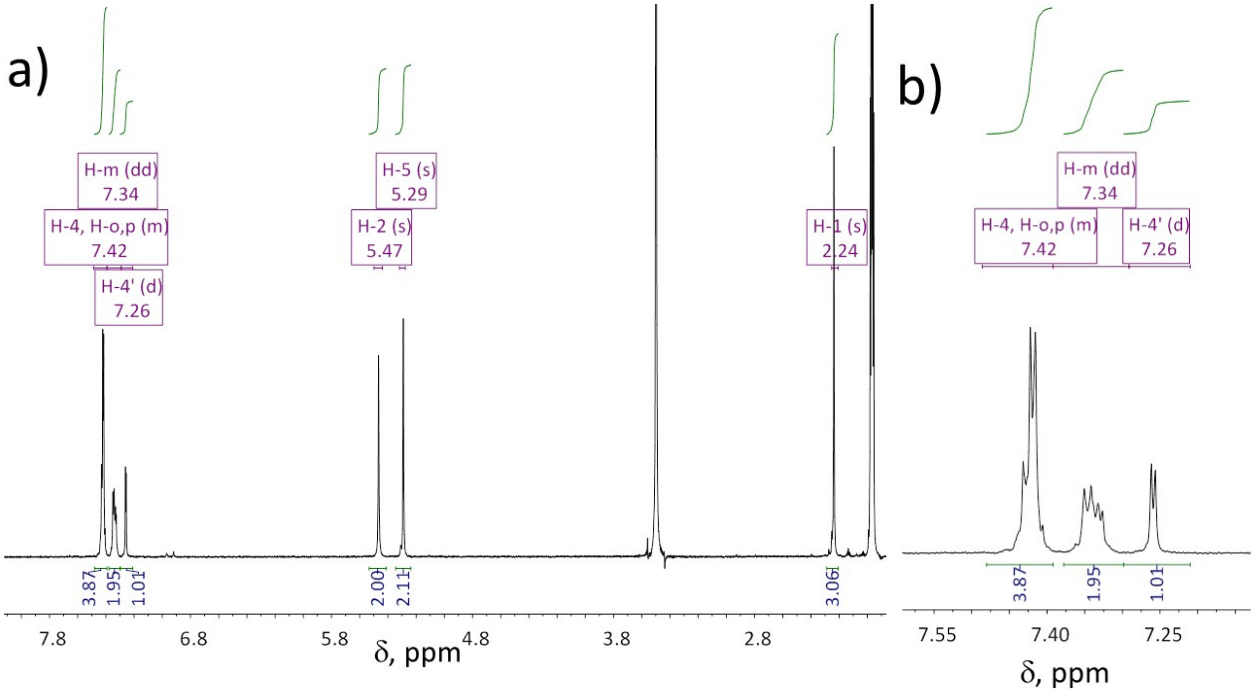

Figure S25: ^{1}H-NMR spectrum of **2**$(PF_6)_3$ in CD_3CN/D_2O 4:1: a) full spectrum, b)zoom of the aromatic region (initial spectrum of the titration shown in Fig. S8).

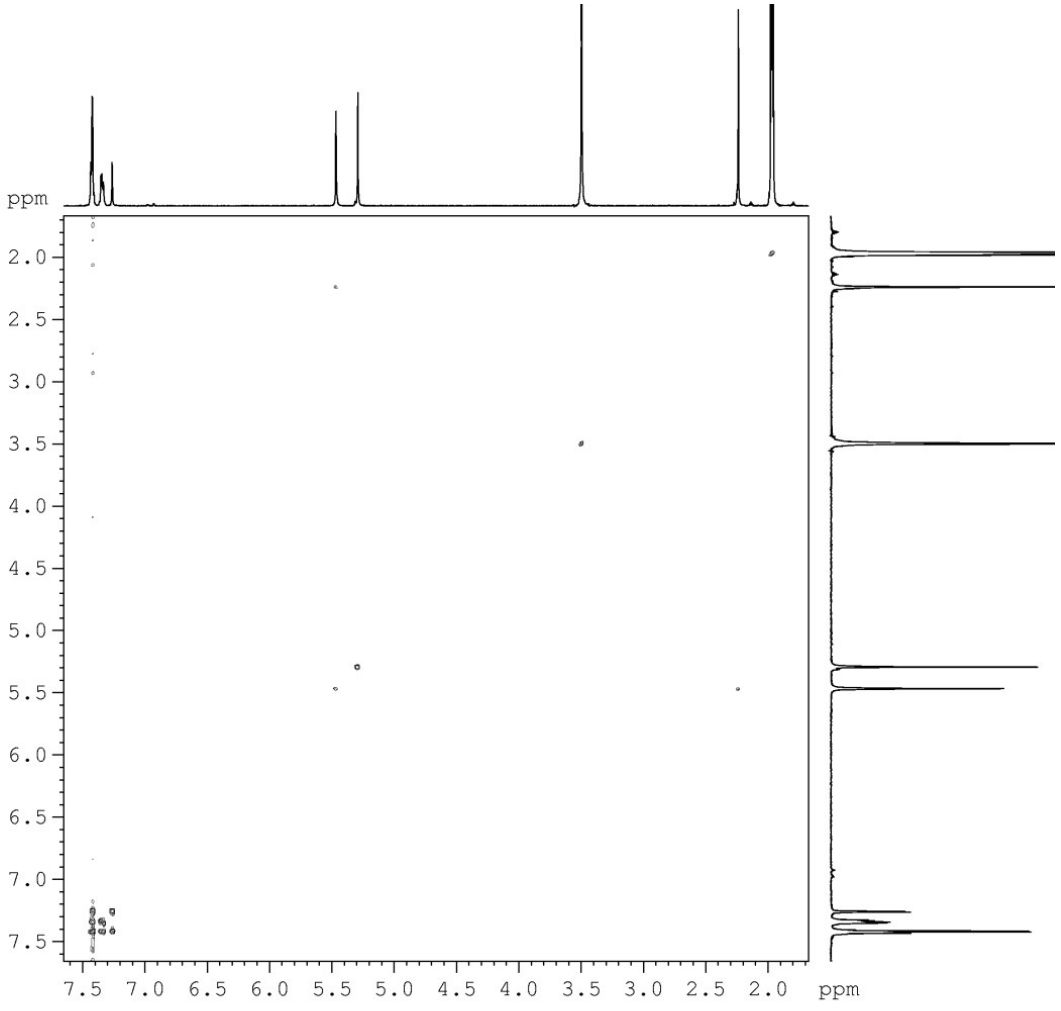

Figure S26: COSY spectrum of **2**$(PF_6)_3$ in CD_3CN/D_2O 4:1 (v/v)

References

[1] G. Bergamaschi, M. Boiocchi, E. Monzani and V. Amendola, *Org. Biomol. Chem*., 2011, **9**, 8276-8283.

[2] P. Gans, A. Sabatini and A. Vacca, *Talanta*, 1996, **43**, 1739-1753.

[3] L.J. Farrugia, *J. Appl. Crystallogr*., 1999, **32**, 837-838.

[4] A.C.T. North, D.C. Phillips and F.S. Mathews, *Acta. Crystallogr*., 1968, **A24**, 351-359

[5] A. Altomare, M. C. Burla, M. Camalli, G. L. Cascarano, C. Giacovazzo, A. Guagliardi, A. G. Moliterni, G. Polidori and R. J. Spagna, *J. Appl. Crystallogr*., 1999, **32**, 115-119

[6] G. M. Sheldrick, *Acta Crystallogr*., 2008, **A64**, 112-122

[7] P. S. Sharma, T. Payagala, E. Wanigasekara, A. B. Wijeratne, J. Huang, D. W. Armstrong, *Chem. Mater*., 2008, **20** (13), 4182–4184.

[8] (a) J. P. Foster, F. Weinhold, *J. Am. Chem. Soc.*, 1980, **102**, 7211−7218; (b) A. E. Reed, R. B. Weinstock, F. Weinhold, *J. Chem. Phys.*, 1985, **83**, 735−746.